Real-Time Observation of Multiple Protein Complex Formation with Single-Molecule FRET

Woori Bae, Mal-Gi Choi, Changbong Hyeon, Yeon-Kyun Shin* and Tae-Young Yoon**

Supporting information

Table of contents

Supplementary Text

Supplementary Methods

Protein expression, purification and labeling. All SNARE proteins were expressed in the *E. coli* Rosetta (DE3) pLysS (Novagen) cell strain. Cells containing GST-tagged yeast membrane SNARE proteins (Snc2p and Sso1pHT (Habc stuncated Sso1p)) (Ref. [1]) were grown at 37°C in LB medium with ampicillin (100 μg/ml) and chloramphenicol (25 μg/ml) until the absorbance at 600 nm (A600) reached 0.6-0.8. Isopropyl-β-D-thiogalactopyranoside (IPTG) was added to a final concentration of 0.5 mM, and the cells were grown at 16°C overnight. The cell pellets were collected by centrifugation at 6,000 x *g* for 10 min and resuspended in 10 ml PBS (pH 7.4) containing 0.2% Triton X-100 (PBST), 1% lauroylsarcosine, 2 mM 4-(2-aminoethyl)-benzenesulfonyl fluoride (AEBSF), and 5 mM DTT. The cells were lysed by sonication on ice and centrifuged at 15,000 x *g* for 30 min at 4°C. The cell lysate was mixed with 1.5 ml of glutathione-agarose beads and nutated for 1 h at 4°C. After binding, the beads were washed extensively with PBST and equilibrated with PBS with 0.8% O.G. The proteins were then cleaved by thrombin (30 U) for 1 h at room temperature.

Cells containing His6-tagged Sec9c were grown at 37°C in LB medium with kanamycin (30 μg/ml) and chloramphenicol (25 μg/ml) until the A600 reached 0.6-0.8. After the addition of IPTG (0.5 mM), the cells were grown further for 4 hrs at 16°C. The cell pellets were collected by centrifugation and resuspended in lysis buffer (20 mM Tris·HCl, 300 mM NaCl, 20 mM imidazole, and 2 mM AEBSF). After sonication followed by centrifugation, the cell lysate was mixed with 1.5 ml Ni-NTA beads and nutated for 1 h at 4°C. After binding, the beads were washed extensively with wash buffer (20 mM Tris·HCl, 300 mM NaCl, and 20 mM imidazole), and the proteins were eluted from the beads with elution buffer (20 mM Tris·HCl, 100 mM NaCl, and 200 mM imidazole). The purity of the proteins was determined by SDS-PAGE.

To label the proteins, the cysteine mutants were treated with a 100-fold molar excess of Tris-(2-carboxethyl) phosphine (TCEP) for 10 min at room temperature and then mixed with Cy3- or Cy5-maleimide (Amersham) at 4°C overnight. The free dye was removed using

a PD-10 desalting column (Amersham). If labeling efficiency was lower than 70%, proteins were labeled one more time with the same protocol.

Vesicle reconstitution. All purified lipid molecules were purchased from Avanti Polar Lipids, except the lipidic dyes DiI (1,1'-dioctadecyl-3,3,3',3'-tetramethylindocarbocyanine perchlorate) and DiD (1,1'-dioctadecyl-3,3,3',3'-tetramethylindodicarbocyanine perchlorate), which were purchased from Invitrogen. Lipid molecules in organic solvent were mixed in cleaned vials using glass GASTIGHT® Syringes (Hamilton) with a 15:65:20 molar ratio of 1,2-dioleoyl-sn-glycero-3-phospho-L-serine (DOPS):1-palmitoyl-2-oleoyl-sn-glycero-3-phosphocholine (POPC):cholesterol. For surface-attached vesicle experiments, 0.1 mol% of biotin-DPPE lipid was added to the lipid solution. For the lipid mixing experiments, 1.8 mol% of DiI and 1.8 mol% DiD were added to the lipid solution for membrane labeling. The lipid solution was completely dried using nitrogen gas and further dried with a vacuum pump for at least 4 hours. The dried lipid film was hydrated with dialysis buffer (25 mM HEPES, 100 mM KCl, 5% glycerol, pH 7.4 using KOH) with a final lipid concentration of 10 mM. Octyl-β-D-glucopyranoside (OG) was added to the lipid solution with final concentration of 1% to solubilize lipid molecules into detergent-lipid micelles. The lipid solution was mixed with protein at a typical molar ratio of 500:1 and then diluted 2 times with dialysis buffer to the lower detergent concentration below the critical micelle concentration. This vesicle solution was dialyzed overnight with 1 L of dialysis buffer containing 2 g of SM2 beads (Bio-Rad) using a dialysis tube with 14kD cut (GEBA). To obtain different numbers of proteins reconstituted in a vesicle, protein concentrations were varied during the reconstitution process (Supplementary Fig. 3).

Single-vesicle fluorescence imaging and experimental determination of FRET value. A quartz slide was coated with 99:1 (mol/mol) mPEG/biotin-PEG (Laysan). The PEG slide was incubated with 0.1 mg/ml of NeutrAvidin (Molecular Probes, Invitrogen) solution for 5 minutes. The t-vesicles, containing biotin-DPPE and Sso1pHT protein, were attached on the PEG layer using biotin-NeutrAvidin binding. The concentration of t-vesicles was adjusted to obtain roughly 10,000 vesicle immobilization per 45×90 μm^2 field of view (Supplementary Fig. 4). This gave the average distance between surface-immobilized vesicles of 640nm, large

enough to prevent interaction of one diffusing vesicle with multiple vesicles on surface. A solution with 1 μM of Sec9c and 20 μM of v-vesicles (reconstituted with Cy3-labeled Snc2p) containing oxygen scavenging system and Trolox[2] was injected through microfluidic buffer exchange. Fluorescence signals from the entire field of view were imaged using a homebuilt wide-field total internal reflection (TIR) microscope (IX71, Olympus). Details of this TIR microscope system were described elsewhere[3]. Briefly, 532-nm TIR excitation was obtained using a Pellin-Broca prism (CVI laser). The fluorescence signal was first filtered with a 550 nm long-pass filter. Two-color images were subsequently produced by a dual-view alignment, in which a 630 nm dichroic mirror (Chroma) separated the fluorescence signals into the Cy3- and Cy5-channels. These two-color images were recorded in parallel with a time resolution of 200 ms, using an electron-multiplying charge-coupled device (Andor). From real-time movies, individual single vesicle-vesicle complexes were identified and their fluorescence intensities were extracted using a custom IDL (ITT Visual Information Solutions) program, which used a Gaussian mask to reduce noise. MATLAB (MathWorks) programs were used to generate the real-time traces. The Cy3- and Cy5-channel signals were re-calibrated by considering the incomplete separation of the Cy3 and Cy5 emission by the dichroic mirror used. Direct excitation of Cy5 and nonspecific background signal before a Cy3 vesicle arrival was calibrated by subtracting average intensity before vesicle arrival. The FRET value E_{tot} was subsequently calculated using the intensity-based equation $E_{tot} = \frac{I_{A,tot}}{I_{D,tot} + I_{A,tot}}$ where $I_{A,tot}$ and $I_{D,tot}$ are the total fluorescence intensities of Cy3 and Cy5 dyes, respectively.

FRET efficiency of single vesicle-vesicle complex in the presence of multiple donor and acceptor dyes

The FRET efficiency of multi-dye system can be formally written as

$$E_{tot} = \frac{k_T}{k_T + \sum_i^{N_D} \tau_{D,i}^{-1}} \qquad (1)$$

The kinetic rate $\tau_{D,i}^{-1}$ represents donor-only processes, including donor fluorescence emission, internal conversion, and intersystem crossing. The total Förster energy transfer rate,

k_T, from N_D donors to N_A acceptors with Förster radius R_0 and interaction potential $\varepsilon(r)$ can be written as

$$k_T = \sum_{i}^{N_D}\sum_{j}^{N_A}\tau_0^{-1}(R_0/r_{ij})^6 = \tau_0^{-1}\sum_{i=1}^{N_D}\left(\int_{|r-\sigma|\le\Omega} d\vec{r} \quad \int_{|r-\sigma|>\Omega} \quad \right) \quad (r)$$

$$\approx \tau_0^{-1}\left[n_D \int_{r_{\min}<r<\sigma+\Omega} d\vec{r} \quad 4\pi\sigma^2 \quad \int_{r>\sigma+\Omega} \quad \right] \qquad (2)$$

where r_{ij} is the inter-dye distance between ith donor and jth acceptor, n_D is the number of bound donor molecules and β is the thermodynamic beta defined as $1/k_BT$. We changed the discrete summation over acceptor positions into a spatial integration over donor-acceptor distance (r) with a Boltzmann weight $p(r) \sim \exp[-\beta\varepsilon_{int}(r)]$. As recapitulated by the crystal structure of the SNARE complex, we presume the Boltzmann weight $p(r)$ sharply peaks near specific position $r = \sigma$ with the amplitude proportional to $e^{\beta\varepsilon_0}$ and is a fast-decaying function beyond an interaction range $(r - \sigma) > \Omega$.

When only n_D out of total N_D donors are in the complex-assembled state, each n_D donor has one acceptor dye stably maintained at the interaction range of σ due to the 1:1 stoichiometric interaction. The integration for the total FRET transfer rate k_T is decomposed into the two contributions from these n_D donors and the remaining N_D - n_D donors,

$$\begin{aligned} k_T &\approx n_D\tau_0^{-1}(R_0/\sigma)^6 e^{\beta\varepsilon_o} + (N_D - n_D)\tau_0^{-1}(R_0/\sigma)^6 e^{\beta\varepsilon_o} q \\ &= n_D\tau_{AD}^{-1} + (N_D - n_D)\tau_A^{-1} \end{aligned}, \qquad (3)$$

where $\tau_{AD}^{-1} \equiv \tau_0^{-1}(R_0/\sigma)^6 e^{\beta\varepsilon_0}$ and $\tau_A^{-1} \equiv \tau_{AD}^{-1} q$ with $q \equiv \dfrac{\int_{(r-\sigma)>\Omega} d\vec{r}(R_0/r)^6 p(r)}{(R_0/\sigma)^6 e^{\beta\varepsilon_0}}$. In particular, q corresponds to the ratio of the fluorescence emission rate of acceptor dyes when the donor has only non-specific interactions with acceptors (τ_A^{-1}) to that when the donor has one stable acceptor partner due to the specific protein-protein interaction (τ_{AD}^{-1}). It should be noted that q << 1 due to the fast-decaying property of $p(r)$ and $(R_0/\sigma)^6 >> 1$, as well as $e^{\beta\varepsilon_0} >> 1$. The kinetic rate for donor emission can be similarly expressed as

$\sum_i^{N_D} \tau_{D,i}^{-1} \approx n_D \tau_{DA}^{-1} + (N_D - n_D)\tau_D^{-1}$, with τ_{DA}^{-1} and τ_D^{-1} denoting the donor fluorescence emission rates in the presence and absence of acceptor dyes, respectively, in the specific interaction range of $|r - \sigma| < \Omega$.

Because the photon number and concomitant signal intensity are proportional to the emission rate ($\tau_\xi^{-1} \propto I_\xi$), one can rewrite the total FRET efficiency in the following form using intensities instead of emission rates:

$$E_{tot} = \frac{n_D I_{AD} + (N_D - n_D) I_A}{n_D I_{AD} + (N_D - n_D) I_A + n_D I_{DA} + (N_D - n_D) I_D}$$

$$= \frac{\left[\frac{n_D}{N_D} + \left(1 - \frac{n_D}{N_D}\right) q\right]\left(\frac{I_{AD}}{I_{AD} + I_{DA}}\right)}{\frac{n_D}{N_D} + \left(1 - \frac{n_D}{N_D}\right)\left(\frac{I_{AD}\{(1-q)/\gamma + q\} + I_{DA}}{I_{AD} + I_{DA}}\right)} \qquad (4)$$

where γ ($= \frac{I_{AD} - I_A}{I_D - I_{DA}}$) is the gamma correction factor for the FRET dye pair. Because $q \ll 1$ in our experimental condition, the above equation is simplified as:

$$E_{tot} = \frac{\left[\frac{n_D}{N_D}\right]\left(\frac{I_{AD}}{I_{AD} + I_{DA}}\right)}{\frac{n_D}{N_D} + \left(1 - \frac{n_D}{N_D}\right)\left(\frac{I_{AD}/\gamma + I_{DA}}{I_{AD} + I_{DA}}\right)} \qquad (5)$$

Analysis of multiple protein-protein FRET traces. A custom MATLAB program used a Schwartz information criterion (SIC) minimization algorithm to identify stepwise changes implicit in the experimentally observed FRET traces. Details of SIC minimization theory and its performance are described elsewhere[4]. We generated step fitted data as follows:

Our goal is to find the optimum set of step positions which minimizes SIC function given as follow :

$SIC = (s+2) \log d + d \log \sigma^2 + d \log 2\pi + d$

Here s is the number of steps, d is the number of data points and σ is standard deviation of original data from step-fitted data. For given set of step positions ($p_1..p_s$), height of

each step is calculated as (h_1 = mean(p_1 to p_2), h_2 = mean(p_2 to p_3)….) for the step-fitted data.

(1) SIC value with a new step position is calculated for every possible step position (in our case, every data point).

(2) We choose a new step position with the lowest SIC value.

New step point is accepted only if addition of the step had decreased SIC. If SIC is not decreased by addition of new step, step finding process is terminated. Otherwise, we continue to find one more step. As new step position is added, step data becomes more close to the original data and $\underline{\sigma}$ decreases. However, (s+2) log d adds constant penalties to SIC upon addition of a step. Thus, if addition of one more step does not decrease STD enough to compensate the penalty, the SIC value is increased. As a result, we obtain the set of step positions that gives the local minimum of SIC.

After the step positions were determined (Fig. 2a, bottom panel, red line), we made estimates for the number of donor-labeled proteins in the vesicle-vesicle complex of interest (N_D) based on fluorescence intensity of single vesicle complex. Because excitation profile of microscopy system gave 16% of error, we draw theoretical FRET states for the several potential N_D values which were compared to the step-fitted FRET data (Fig. 2a, bottom panel, green arrows). We finally determined N_D that gives the best match between the step-fitted FRET data and the theoretical FRET states (For example, see how different N_D values give different FRET value sets in Fig. 2a). We extracted the number and the timing of SNARE complex formation by comparing the step-fitted FRET data with the theoretical FRET states.

Signal-to-noise ratio. To quantitatively understand the change in SNR with an increasing N_D, we considered the numbers of photons in the donor channel m_D and acceptor channel m_A recorded during our time resolution[5]. Because the total FRET of a vesicle-vesicle complex is measured as $E_{tot} = \frac{m_A}{m_A + m_D}$, fluctuation of E_{tot} originates in part from the shot noise of these photon numbers. In the case of low photon numbers, we need to consider the exact joint probability distribution for getting m_A and m_D;

$$P\left(E_{\text{tot}} \mid t=200ms\right)=\sum_{\substack{m_A,m_D \\ m_A+m_D\geq m_\tau}}^{\infty} P\left(m_A m_D \mid t=200ms\right)\delta\left(E_{\text{tot}}-\frac{m_A}{m_A+m_D}\right)$$

$$=\frac{\sum_{\substack{m_A,m_D \\ m_A+m_D\geq m_\tau}}^{\infty} \frac{\left[\alpha M\right]^{m_A}}{m_A!}\frac{\left[\left(1-\alpha\right)M\right]^{m_D}}{m_D!}e^{-M}\delta\left(E_{\text{tot}}-\frac{m_A}{m_A+m_D}\right)}{\sum_{\substack{m_A,m_D \\ m_A+m_D\geq m_\tau}}^{\infty} \frac{\left[\alpha M\right]^{m_A}}{m_A!}\frac{\left[\left(1-\alpha\right)M\right]^{m_D}}{m_D!}e^{-M}} \quad (6)$$

where α is the mean FRET value, M is the mean photon number from a FRET pair and m_τ is the minimum photon number required to pass our detection criteria. The denominator is simplified to $\sum_{\substack{m_A,m_D \\ m_A+m_D\geq m_\tau}}^{\infty} \frac{\left[\alpha M\right]^{m_A}}{m_A!}\frac{\left[\left(1-\alpha\right)M\right]^{m_D}}{m_D!}e^{-M}=e^{-M}\sum_{j=m_\tau}^{\infty}\frac{M^j}{j!}$. We can calculate the measurement noise due to this shot noise, $\left\langle\left(\delta E_{\text{tot}}\right)^2\right\rangle=\sigma_p^2$, using the above probability distribution. This gives ${\sigma_p}^2=\alpha\left(1-\alpha\right)\Psi_p\left(M\right)$, where $\Psi_p\left(M\right)=\sum_{j=m_\tau}^{\infty}\frac{M^j}{j!j}\Big/\sum_{j=m_\tau}^{\infty}\frac{M^j}{j!}$. Because our vesicle-vesicle complex contains N_D donor dyes, $\Psi_p\left(M\right)$ is modified to $\Psi_p\left(N_D\right)=\sum_{j=m_\tau}^{\infty}\frac{\left(MN_D\right)^j}{j!j}\Big/\sum_{j=m_\tau}^{\infty}\frac{\left(MN_D\right)^j}{j!}$. We then include a constant background noise of σ_D, which arises from the dark current noise of our imaging apparatus. The total FRET fluctuation, including both shot noise and dark current, is given as ${\sigma_{total}}^2=\left(\sigma_p\left(N_D\right)\right)^2+\sigma_D^2$. The SNR of our multiple protein-protein FRET measurement is thus given as:

$$SNR\left(N_D\right)=\frac{H/N_D}{\sigma_{total}\left(N_D\right)}. \quad (7)$$

With SNR value of 2, about 80% of real step is located within 3 data points of detected step position. So we chose 1sec (5 times of our 200ms time resolution) as histogram bin of dwell time distribution (Fig. 4a).

Supplementary Text

Single-vesicle system

We used single-vesicle system to study binding kinetics of membrane protein, SNARE in molecular crowded environment where cooperative membrane protein interaction comes into play. However, such crowded environment often demands presence of hundreds of target molecules per diffraction limited spot (usually several hundreds of nanometer) of imaging system which makes single molecule experiments practically impossible. We solved this problem by compartmentalizing crowded proteins into different vesicles immobilized farther than diffraction limit. Then signal from one diffraction limited spot (one vesicle) should originate from only several proteins and single molecule analysis becomes feasible. This condition is achieved in single-vesicle system by limiting number of diffusing vesicles and thereby limiting number of vesicle-vesicle complex by several hundred per field of view (FOV, 45×90 μm^2). Number of proteins in single vesicle (N_D) is conserved throughout the reaction and we used this property to define FRET substates of each vesicle complex.

Experimental parameters should be carefully determined to prepare proper sample in vesicle system to study a membrane protein. For example, we prepared vesicles with only one protein to measure control parameters γ and H with single molecule FRET traces (Fig. 1c and Supplementary Fig. 5) and we prepared vesicles with 10 proteins to observe multimeric interaction in SNARE complex formation. Although we cannot precisely control the number of protein per vesicle because of stochastic nature of reconstitution process, we can control the average number of proteins in one vesicle by changing protein concentration during reconstitution process (Supplementary Fig. 3). Number of proteins per vesicle was determined by detecting photobleaching step. We used 0.5μM of protein to prepare one-SNARE vesicle and 8μM of protein to prepare 10-SNARE vesicle.

We used detergent depletion method after solubilization of lipid to prepare proteoliposome[6] which is widely used in many in-vitro vesicle fusion studies[7-9]. Due to stochastic nature of protein insertion and vesicle formation, careful data interpretation is required when using this method. For example, vesicle preparation after solubilization produces about 80% of outer faces protein[10] and protein distribution in vesicle can be also inhomogeneous[11]. Former effect reduces number of possible protein complexes and this means our cooperative SNARE complex formation is even underestimated result. Heterogeneity of protein number in one

vesicle is much tricky to consider because vesicle size and lipid composition[12] also bears intrinsic heterogeneity. We however observed that at least 59% of SNARE complex assembly shows simple first-order binding kinetics in such heterogeneous environment (Fig. 2d, populations other than first bin). Of course, heterogeneity in protein concentration[13] and lipid composition[14] may facilitate cooperative SNARE complex formation and following vesicle fusion.

Labeling efficiency of SNARE proteins

Incomplete labeling efficiency hinders detection of SNARE complex formation. Although many attempts to enhance the efficiency of attaching organic dyes to target proteins were made, 100% labeling was still not an easy task[15] especially for membrane protein. Therefore, many single molecule studies employs techniques like alternating laser excitation (ALEX) to identify proper labeled FRET pair. This technique however, is not applicable in our system where 70% of labeling efficiency and 10 molecules in single vesicle complex gives only 0.7^{10} = 3% of probability for complete single vesicle labeling. Thereby most of our vesicles have dark proteins and corresponding protein complexes remain undetected throughout the experiment. We cannot recover original number of protein in each vesicle because of stochastic nature of labeling and protein incorporation procedure. However, we can recover distribution of protein and complex number by referring negative binomial distribution. The negative binomial distribution is the discrete probability of a distribution's success until a certain number of failures occur. In our case, we can calculate the probability of unlabeled protein number once we know the number of labeled protein. For example, if we detected 3 Cy3 molecules, with a labeling efficiency of 70% (probability of unlabeled is 30%), the probability function for an unlabeled protein can be written as NB(3, 0.3). We can convert the experimental distribution to the original distribution by using this probability mass function (Supplementary Fig. 8 from black bars to red bars).

Supplementary Figures

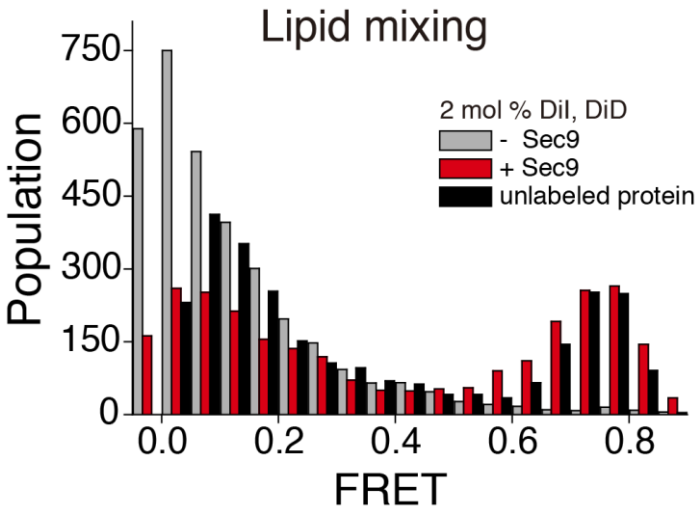

Supplementary Figure 1. Single vesicle membrane fusion activity test on labeled protein. To ensure that our labeling did not interfere with the functionality of SNARE proteins, the v- and t-vesicles were additionally labeled with 2 mol% of 1,1′-dioctadecyl-3,3,3′,3′-tetramethylindocarbocyanine perchlorate (DiI) and 1,1′-dioctadecyl-3,3,3′,3′-tetramethylindodicarbocyanine perchlorate (DiD), respectively for membrane fusion assay. Although individual Cy3 and Cy5 molecules are brighter than DiI and DiD because of their higher quantum yields (0.15 versus 0.07), these membrane dyes far outnumbered the protein-labeling Cy3 and Cy5 dyes (400 versus 10). Thus, the fluorescence signal from these additionally labeled vesicles mainly reported membrane rearrangements inside single vesicle-vesicle complexes. Membrane merging between the two vesicles led to the mixing of DiI and DiD, which resulted in an increased energy transfer from DiI to DiD (Ref [16]). After a 10 min reaction at 37°C, unbound v-vesicles and Sec9c proteins were removed by microfluidic buffer exchange. We were able to observe the formation of hundreds of single vesicle-vesicle complexes per FOV (45×90 μm^2). When we studied the FRET efficiency of thousands of individual single-vesicle complexes, we were able to observe a high FRET peak centered at 0.7, the hallmark of membrane merging although some vesicles still remained only at docking state with FRET value centered on 0.1 similar to result with unlabeled SNARE proteins. When the same reaction was repeated without Sec9c, this high FRET peak totally disappeared, and the majority of the single-vesicle complexes remained in the low FRET region, below 0.25. FRET histogram using unlabeled protein gave similar result (black bar).

This confirms that the functionality and specificity of SNARE proteins remain intact after labeling with organic dyes.

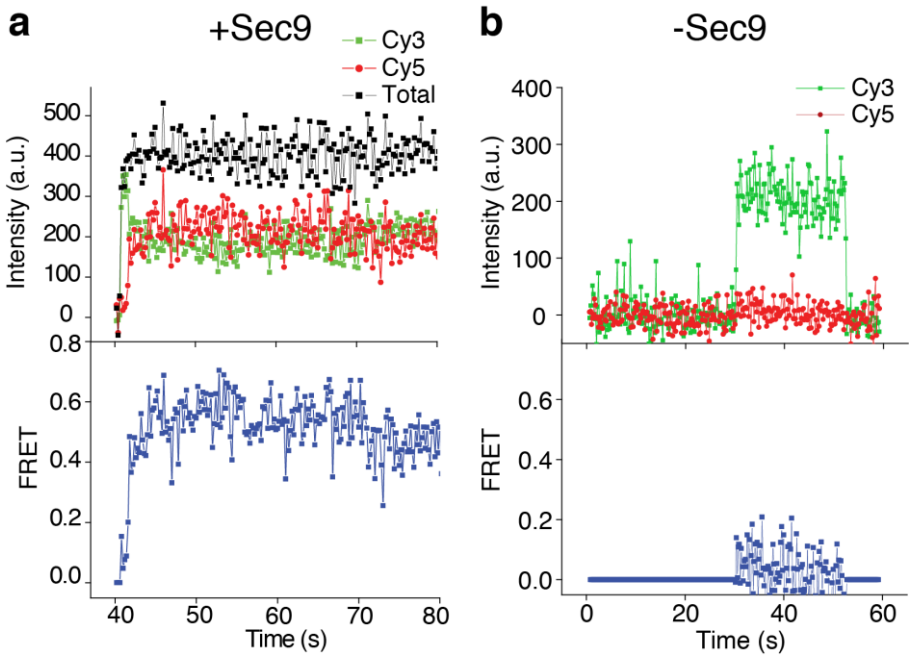

Supplementary Figure 2. Dependence of the single-vesicle FRET data on the complete set of SNARE proteins. (**a**) Only in the presence of soluble Sec9c, which constitutes a complete SNARE set with Sso1pHT (in t-vesicles) and Snc2p (in v-vesicles), a strong FRET signal was observed subsequent to single vesicle-vesicle docking event. (N_D= 5) (**b**) When Sec9c was omitted from the reaction solution, only was transient docking of single vesicle without a FRET increase observed. (N_D= 4) These observations importantly demonstrate that the FRET signal was selectively generated by the complete SNARE complexes.

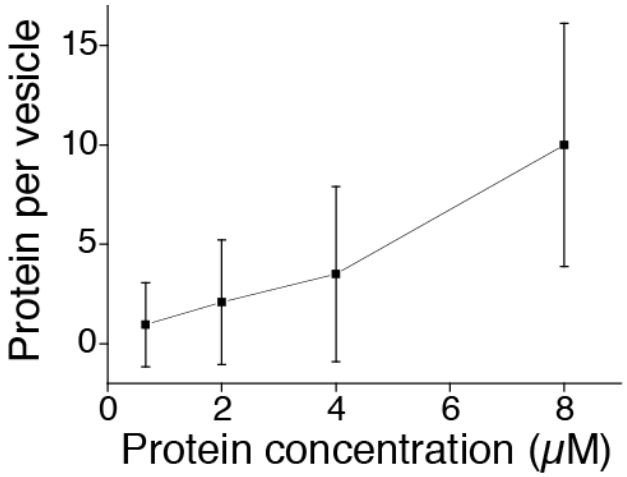

Supplementary Figure 3. Number of Snc proteins per vesicle as a function of Snc concentration used for reconstitution. To see whether we could control the number of reconstituted proteins per vesicle, we varied the Snc concentration during the reconstitution process. The average number of Snc per vesicle was measured through the number of photobleaching steps observed for single vesicles. In general, the average number of Snc per vesicle linearly increased with the Snc concentration used. When we used a higher concentration of 8 μM, the increase slope was slightly deflected, which may hint about a cooperative behavior in protein reconstitution. Based on this experiment, we used different protein (Snc and Sso) concentrations, for example, 0.5 μM for studying the case of N_D=1 to obtain γ and H values and 8 μM for observing multimeric SNARE complex formation events.

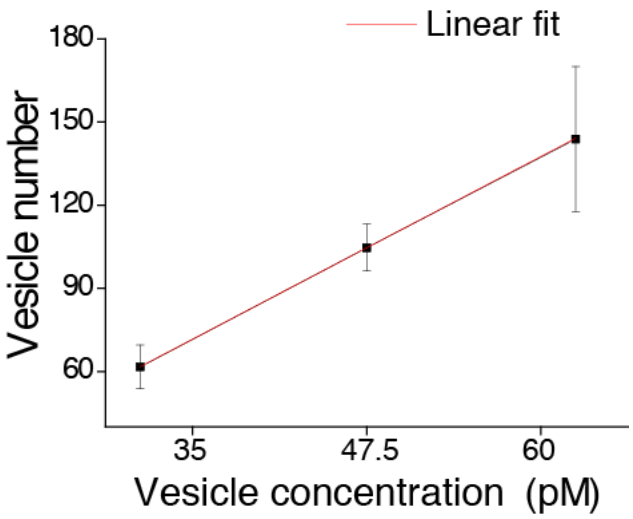

Supplementary Figure 4. Number of surface-immobilized t-vesicles per FOV. We counted the number of immobilized t-vesicles per FOV (using 633 nm excitation) after using lower concentrations for t-vesicle incubation with surface. Concentration of t-vesicle was estimated from lipid concentration by assuming ~30nm diameter vesicle. The immobilization number linearly increased with the t-vesicle concentration used for incubation. When this linear trend was extrapolated up to a t-vesicle concentration of 1.5 nM, which was used for the main FRET measurements, it was estimated that there were approximately 10,000 t-vesicles per FOV (45×90 μm^2). This gives an inter-t-vesicle distance of 640nm on average, which is large enough to prevent one diffusing v-vesicle (~30 nm diameter) from interacting with multiple t-vesicles on surface. Error bar indicates standard deviation from 15 images.

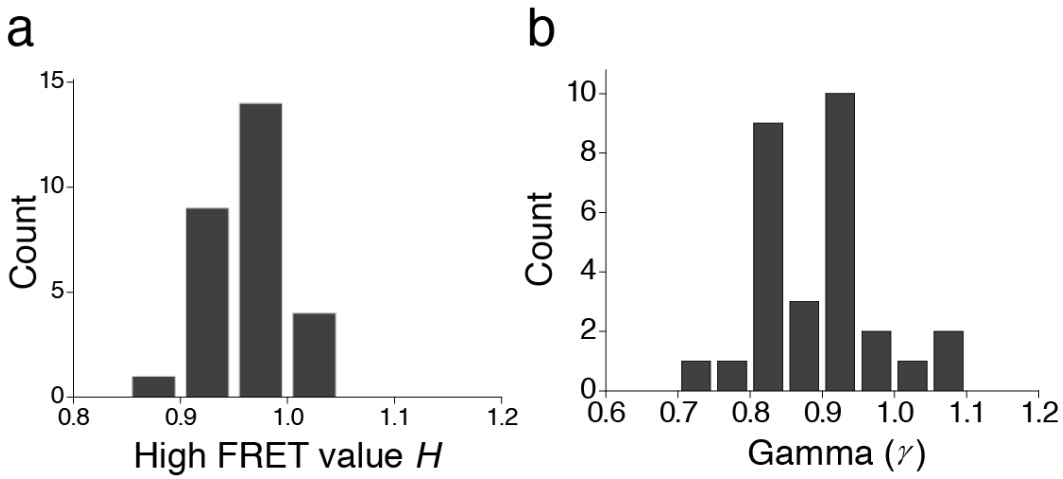

Supplementary Figure 5. Distributions of high FRET value (*H*) and gamma correction factor (γ). Distribution of 30 molecules gives mean values of 0.96 and 0.89 and the standard deviations of 0.037 and 0.075 for *H* and γ, respectively. The standard deviation of γ is about two times larger than that of *H*. This is because the standard deviation of *H* measures linear error in the FRET value of a single vesicle complex, whereas the standard deviation of γ gives $1/\gamma$ error. Since both values are close to 1 in our experiment, deviation of these values gives similar degree of error.

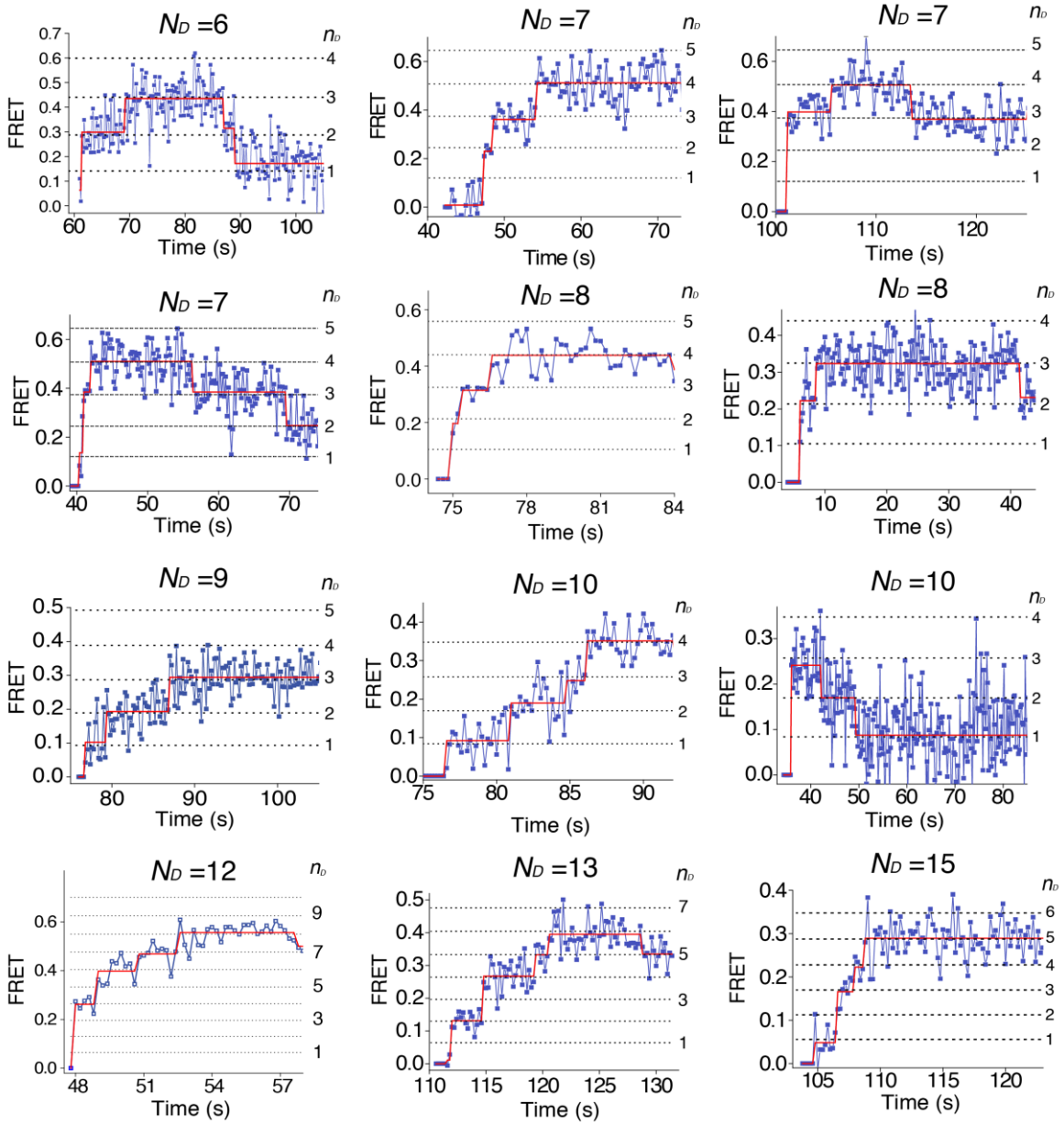

Supplementary Figure 6. Sample real-time traces of multiple protein-protein FRET signals. Blue traces are original FRET data, and red lines are step-fitted data. Black dashed lines are the calculated theoretical FRET value. The estimated N_D value is specified for each trace.

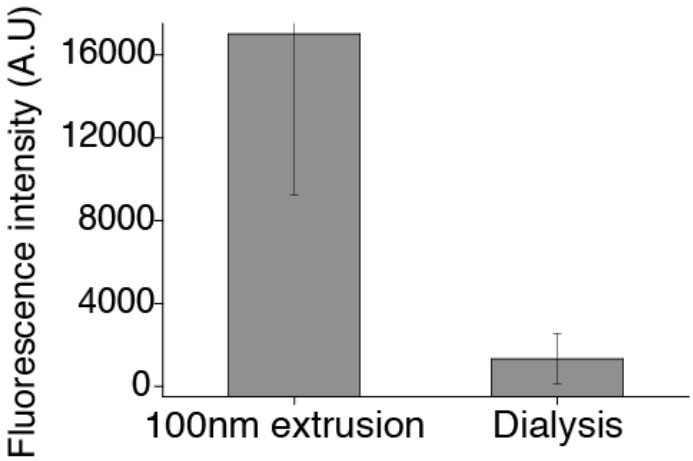

Supplementary Figure 7. Fluorescence intensity of 100nm vesicle and proteoliposome. We characterized the size of dialyzed vesicle by comparing fluorescence intensity of dialyzed vesicle to that of 100nm sized vesicle produced by extrusion. Average intensity of dialyzed vesicle was 1330 while intensity of 100nm vesicle was 17000. By calculating square root of intensity ratio, we got 3.58 times smaller dialyzed vesicle. Its diameter was 28nm.

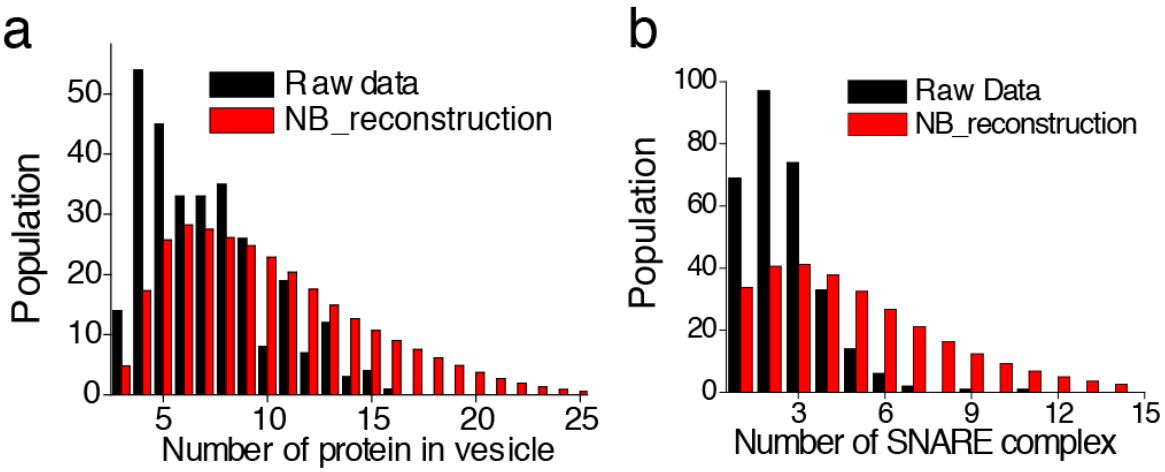

Supplementary Figure 8. Number of protein molecules in one vesicle and number of SNARE complexes in one vesicle complex. (**a**) The number of v-SNARE protein molecules in one vesicle. The red bars are reconstructed data using a negative binomial distribution. We can use a negative binomial to correct for the incomplete labeling efficiency (70%) with the assumption that labeling does not interfere with the reconstitution process. (**b**) Number of SNARE complex molecules in one vesicle complex. The red bars are negative binomial reconstruction data.

Supplementary References

(1) Zhang, F.; Chen, Y.; Su, Z.; Shin, Y.-K. *J. Biol. Chem.* **2004**, *279*, 38668.

(2) Roy, R.; Hohng, S.; Ha, T. *Nat. Methods* **2008**, *5*, 507.

(3) Joo, C.; McKinney, S. A.; Nakamura, M.; Rasnik, I.; Myong, S.; Ha, T. *Cell* **2006**, *126*, 515.

(4) Kalafut, B.; Visscher, K. *Comput Phys Commun* **2008**, *179*, 716.

(5) Gopich, I.; Szabo, A. *J. Chem. Phys.* **2005**, *122*, 14707.

(6) Lasic, D. D. *Biochem. J.* **1988**, *256*, 1.

(7) Kyoung, M.; Srivastava, A.; Zhang, Y.; Diao, J.; Vrljic, M.; Grob, P.; Nogales, E.; Chu, S.; Brunger, A. T. *Proc. Natl. Acad. Sci. U. S. A.* **2011**, *108*, E304.

(8) Hernandez, J. M.; Stein, A.; Behrmann, E.; Riedel, D.; Cypionka, A.; Farsi, Z.; Walla, P. J.; Raunser, S.; Jahn, R. *Science* **2012**, *336*, 1581.

(9) Karatekin, E.; Rothman, J. E. *Nat. Protoc.* **2012**, *7*, 903.

(10) Chen, X.; Arac, D.; Wang, T. M.; Gilpin, C. J.; Zimmerberg, J.; Rizo, J. *Biophys. J.*

2006, *90*, 2062.

(11) Christensen, S. M.; Mortensen, M. W.; Stamou, D. G. *Biophys. J.* **2011**, *100*, 957.

(12) Larsen, J.; Hatzakis, N. S.; Stamou, D. *J. Am. Chem. Soc.* **2011**, *133*, 10685.

(13) Sieber, J. J.; Willig, K. I.; Kutzner, C.; Gerding-Reimers, C.; Harke, B.; Donnert, G.; Rammner, B.; Eggeling, C.; Hell, S. W.; Grubmuller, H.; Lang, T. *Science* **2007**, *317*, 1072.

(14) Chamberlain, L. H.; Burgoyne, R. D.; Gould, G. W. *Proc. Natl. Acad. Sci. U. S. A.* **2001**, *98*, 5619.

(15) Kim, Y.; Ho, S. O.; Gassman, N. R.; Korlann, Y.; Landorf, E. V.; Collart, F. R.; Weiss, S. *Bioconjug. Chem.* **2008**, *19*, 786.

(16) Yoon, T. Y.; Okumus, B.; Zhang, F.; Shin, Y. K.; Ha, T. *Proc Natl Acad Sci USA* **2006**, *103*, 19731.